Finite-Resolution DACs Based Hybrid Beamforming Design for Covert Communications

Wei Ci and Chenhao Qi
School of Information Science and Engineering, Southeast University, Nanjing, China
Email: {ciwei,qch}@seu.edu.cn

GLOBECOM 2024 - 2024 IEEE Global Communications Conference | 979-8-3503-5125-5/24/$31.00 ©2024 IEEE | DOI: 10.1109/GLOBECOM52923.2024.10901553

***Abstract*—We investigate hybrid beamforming design for covert multiple-input multiple-output communications with finite-resolution digital-to-analog converters (DACs), which impose practical hardware constraints not yet considered by the existing works and have negative impact on the covertness. Based on the additive quantization noise model, we derive the detection error probability of the warden considering finite-resolution DACs. Aiming at maximizing the sum covert rate (SCR) between the transmitter and legitimate users, we design hybrid beamformers subject to the power and covertness constraints. To solve this nonconvex joint optimization problem, we propose an alternating optimization (AO) scheme based on fractional programming, quadratic transformation, and inner majorization-minimization methods to iteratively optimize the analog and digital beamformers. Simulation results verify the performance gain provided by the proposed AO scheme.**

***Index Terms*—Covert communications, digital-to-analog converter (DAC), hybrid beamforming, multiuser communications.**

I. Introduction

Traditional secure communications primarily focus on preventing messages from being decoded by potential eavesdroppers. However, in specific scenarios such as battlefield environments, even the regular wireless communications can expose us to the enemy and result in fatal danger. This leads to the emergence of covert communication techniques to achieve enhanced security. In a typical wireless covert communication system, a legitimate transmitter aims to communicate with a legitimate user without being detected by a warden. However, for the additive white Gaussian noise (AWGN) channel, the square root law has been proved that only $\mathcal{O}(\sqrt{n})$ bits can be transmitted in n channel uses, indicating that the covert bits per channel use decreases to zero if n grows to be infinity [1]. Therefore, uncertainties such as noise and channel fading are investigated to achieve a positive covert rate [2], [3].

Besides of introducing uncertainties to the wireless communications, we can also mitigate the power leakage to the warden through elaborately designing beamformers [4], [5]. For example, the authors in [4] investigate achieving covertness in both beam training and data transmission stages with a discrete Fourier transform codebook. The zero-forcing and robust beamformers are proposed to maximize the covert rate [5]. Moreover, the advancement of millimeter wave (mmWave) massive antenna arrays leads to the emergence of hybrid beamforming techniques [6], [7], which can also be used for covert communications. A joint hybrid beamformer and jamming design framework is proposed for a covert communication system with a full-duplex receiver, where the detection error probabilities of the warden are derived for both single and multiple data stream cases [8]. However, these works mainly focus on the ideal beamformer design with infinite-resolution digital-to-analog converters (DACs) or analog-to-digital converters (ADCs). On one hand, employing high-resolution DACs or ADCs can result in significant power consumption [9]. On the other hand, using low-resolution DACs or ADCs introduces significant quantization noise, which have negative impact on both the communication performance and covertness.

In this paper, we investigate hybrid beamforming design for covert multiple-input multiple-output (MIMO) communications with finite-resolution DACs, which impose practical hardware constraints not yet considered by the existing works and have negative impact on the covertness. Based on the additive quantization noise model, we derive the detection error probability of the warden considering finite-resolution DACs. Aiming to maximize the sum covert rate (SCR) between the transmitter and legitimate users subject to the power and covertness constraints, we propose an alternating optimization (AO) scheme to design the analog and digital beamformers in an iterative manner. Specifically, for the analog beamformer design subproblem, we transform it into a quadratically constrained quadratic programming (QCQP) problem with an extra constant-modulus constraint and solve it by an inner majorization-minimization (iMM) method. For the digital beamformer design subproblem, we transform it into a standard QCQP convex problem, which is then solved by the interior-point method.

The notations are defined as follows. Symbols for vectors (lower case) and matrices (upper case) are in boldface. $(\cdot)^*$, $(\cdot)^{\mathrm{T}}$ and $(\cdot)^{\mathrm{H}}$ denote the conjugate, transpose and conjugate transpose, respectively. $[\boldsymbol{a}]_n$, $[\boldsymbol{A}]_{m,n}$, $[\boldsymbol{A}]_{:,m}$ and $\|\boldsymbol{A}\|_{\mathrm{F}}$ denote the nth entry of the vector $\boldsymbol{a}$, the entry on the mth row and nth column, the mth column and the Frobenius norm of the matrix $\boldsymbol{A}$, respectively. $\boldsymbol{A} \succeq 0$ indicates that $\boldsymbol{A}$ is a positive semi-definite matrix. $\boldsymbol{I}_L$ denotes an $L \times L$ identity matrix. The functions $\mathrm{vec}(\cdot)$, $\mathrm{vec}^{-1}(\cdot)$, $\mathrm{Tr}(\cdot)$ and $\mathrm{diag}(\cdot)$ denote the vectorization, inverse operation of vectorization, trace and diagonal matrix, respectively. $\mathrm{Re}(\cdot)$ and $\angle(\cdot)$ denote the real part and the angle of a complex-valued number, respectively. $\mathbb{E}(\cdot)$ denotes the statistical expectation. $\mathcal{CN}(\boldsymbol{\mu}, \boldsymbol{\Sigma})$ denotes a complex Gaussian distribution with mean $\boldsymbol{\mu}$ and covariance matrix $\boldsymbol{\Sigma}$. Symbols j, $\mathbb{R}$, $\mathbb{C}$ and $\otimes$ denote the square root of -1, the set of real-valued numbers, complex-valued numbers and the Kronecker product, respectively.

II. System Model And Problem Formulation

A. System Model

We consider a covert mmWave MIMO communication system, where a base station named Alice simultaneously communicates with K legitimate users, meanwhile a warden named Willie attempts to detect the existence of the communications. Alice uses a fully-connected hybrid beamforming architecture with N antennas and N_{RF} radio frequency (RF) chains, where the antennas are placed in uniform linear arrays with half wavelength intervals and each RF chain is connected to a finite-resolution DAC. To reduce the hardware complexity and ensure the performance of massive antenna array communications, we set $N_{\mathrm{RF}} = K \ll N$. The K legitimate users and Willie are all equipped with a single antenna for simplicity.

The transmitted information symbols of K data streams from Alice are firstly precoded by a baseband digital beamformer $\boldsymbol{F}_{\mathrm{B}} \triangleq [\boldsymbol{f}_{\mathrm{B},1}, \cdots, \boldsymbol{f}_{\mathrm{B},K}] \in \mathbb{C}^{K\times K}$, then converted by finite-resolution DACs. The baseband transmitted signal can be expressed as

$$\boldsymbol{x}_{\mathrm{b}} = \mathbb{Q}\Big(\sum_{k=1}^{K} \boldsymbol{f}_{\mathrm{B},k} s_k\Big), \tag{1}$$

where $s_k \in \mathbb{C}$ for $k = 1, 2, \cdots, K$ is the information symbol transmitted to the kth user. $\mathbb{Q}(\cdot)$ denotes the quantization function imposed by the finite-resolution DACs. Additionally, we denote $\boldsymbol{s} \triangleq [s_1, s_2, \cdots, s_k]^{\mathrm{T}} \sim \mathcal{CN}(\boldsymbol{0}, \boldsymbol{I}_K)$, indicating that the symbols from different data streams are independent of each other. To derive a tractable expression for (1), we use the the additive quantization noise (AQN) model [10] to approximate the output with an linear form as

$$\boldsymbol{x}_{\mathrm{b}} \approx (1-\beta)\sum_{k=1}^{K} \boldsymbol{f}_{\mathrm{B},k} s_k + \boldsymbol{\eta}_{\mathrm{q}}, \tag{2}$$

where β is the quantization distortion parameter and it depends on the resolution of the DACs. Let b denote the number of quantized bits of the DACs. Specifically, if we set $b = 1, 2, \cdots, 5$, the values of β are 0.3634, 0.1175, 0.03454, 0.009497 and 0.002499, respectively. When $b > 5$, β can be approximated by $\frac{\pi\sqrt{3}}{2}2^{-2b}$. As b grows to be infinity, β will be 0 and it means that there is no quantization distortion. $\boldsymbol{\eta}_{\mathrm{q}} \in \mathbb{C}^K$ denotes the quantization noise and its covariance matrix can be expressed as

$$\boldsymbol{R}_{\mathrm{q}} = \beta(1-\beta)\mathrm{diag}\Big(\sum_{k=1}^{K} \boldsymbol{f}_{\mathrm{B},k}\boldsymbol{f}_{\mathrm{B},k}^{\mathrm{H}}\Big). \tag{3}$$

After being up-converted to the RF domain, the transmitted signals are precoded by an analog beamformer $\boldsymbol{F}_{\mathrm{R}} \in \mathbb{C}^{N\times K}$. Therefore, the received signal by the kth legitimate user can be expressed as

$$y_k = \boldsymbol{h}_k^{\mathrm{H}}\boldsymbol{F}_{\mathrm{R}}\big(\sum_{l=1}^{K}(1-\beta)\boldsymbol{f}_{\mathrm{B},l}s_l + \boldsymbol{\eta}_{\mathrm{q}}\big) + \overline{\eta}_k, \tag{4}$$

where $\overline{\eta}_k \sim \mathcal{CN}(0, \sigma_k^2)$ denotes the AWGN at the kth legitimate user. $\boldsymbol{h}_k$ denotes the channel vector between Alice and the kth legitimate user and can be expressed as

$$\boldsymbol{h}_k = \sqrt{\frac{N}{D_k}}\Big(\alpha_k^{(0)}\boldsymbol{a}(N, \theta_k^{(0)}) + \sum_{d=1}^{D_k-1}\alpha_k^{(d)}\boldsymbol{a}(N, \theta_k^{(d)})\Big), \tag{5}$$

where D_k denotes the total number of channel paths between Alice and the kth user. $\alpha_k^{(0)}$ and $\alpha_k^{(d)}$ for $d = 1, 2, \cdots, D_k - 1$ denote the channel gain for the line-of-sight (LOS) and the dth non-line-of-sight (NLOS) channel paths, respectively. $\theta_k^{(0)}$ and $\theta_k^{(d)}$ for $d = 1, 2, \cdots, D_k - 1$ denote the channel angle-of-departure (AoD) for the LOS and the dth NLOS channel paths, respectively. Moreover, $\boldsymbol{a}(N, \theta)$ is the normalized array response and can be expressed as

$$\boldsymbol{a}(N, \theta) = \frac{1}{\sqrt{N}}\big[1, e^{j\pi\sin(\theta)}, \cdots, e^{j\pi(N-1)\sin(\theta)}\big]^{\mathrm{T}}. \tag{6}$$

Similarly, the channel vector between Alice and Willie can be expressed as

$$\boldsymbol{h}_{\mathrm{w}} = \sqrt{\frac{N}{D_{\mathrm{w}}}}\Big(\alpha_{\mathrm{w}}^{(0)}\boldsymbol{a}(N, \theta_{\mathrm{w}}^{(0)}) + \sum_{d=1}^{D_{\mathrm{w}}-1}\alpha_{\mathrm{w}}^{(d)}\boldsymbol{a}(N, \theta_{\mathrm{w}}^{(d)})\Big), \tag{7}$$

where $D_{\mathrm{w}}, \alpha_{\mathrm{w}}$ and θ_{w} are distinguished with D_k, α_k and θ_k in (5).

In this paper, we assume that Alice knows the instantaneous CSI of $\boldsymbol{h}_k$ for $k = 1, 2, \cdots, K$, which can be obtained via uplink training for channel estimation. However, Willie is usually a passive node and we assume that only statistical CSI of $\boldsymbol{h}_{\mathrm{w}}$ represented by $\boldsymbol{\Omega}_w$ is available to Alice [8]. Considering the worst case, we assume that Willie knows all the instantaneous CSIs of $\boldsymbol{h}_{\mathrm{w}}$ and $\boldsymbol{h}_k$ for $k = 1, 2, \cdots, K$.

B. Detection Performance of Willie

The signal detection process of Willie can be formulated as a binary hypothesis testing problem. Specifically, hypothesis $\mathcal{H}_0$ represents that Alice remains silent, while hypothesis $\mathcal{H}_1$ represents that Alice is transmitting signals. Then the received signal at Willie in the tth time slot can be derived as

$$\mathcal{H}_0: y_{\mathrm{w}}[t] = \overline{\eta}_{\mathrm{w}}[t], \tag{8}$$

$$\mathcal{H}_1: y_{\mathrm{w}}[t] = \boldsymbol{h}_{\mathrm{w}}^{\mathrm{H}}\boldsymbol{F}_{\mathrm{R}}\big(\sum_{l=1}^{K}(1-\beta)\boldsymbol{f}_{\mathrm{B},l}s_l[t] + \boldsymbol{\eta}_{\mathrm{q}}[t]\big) + \overline{\eta}_{\mathrm{w}}[t], \tag{9}$$

where $\overline{\eta}_{\mathrm{w}}[t] \sim \mathcal{CN}(0, \sigma_{\mathrm{w}}^2)$ denotes the AWGN received by Willie in the tth time slot. For representation simplicity, we define $\mathcal{D}_0$ and $\mathcal{D}_1$ to represent the decisions of Willie under $\mathcal{H}_0$ and $\mathcal{H}_1$, respectively. Therefore, we can derive the detection error probability of Willie as

$$\mathcal{P}_{\mathrm{e}} = \mathcal{P}_{\mathrm{FA}} + \mathcal{P}_{\mathrm{MD}}, \tag{10}$$

where $\mathcal{P}_{\mathrm{FA}} \triangleq \Pr(\mathcal{D}_1|\mathcal{H}_0)$ denotes the false alarm probability and represents that Willie performs inference $\mathcal{D}_1$ but $\mathcal{H}_0$ holds, and $\mathcal{P}_{\mathrm{MD}} \triangleq \Pr(\mathcal{D}_0|\mathcal{H}_1)$ denotes the missed detection probability and represents that Willie performs inference $\mathcal{D}_0$

$$\mathrm{SIQNR}_k=\frac{(1-\beta)^2|\boldsymbol{h}_k^{\mathrm{H}}\boldsymbol{F}_{\mathrm{R}}\boldsymbol{f}_{\mathrm{B},k}|^2}{(1-\beta)^2\sum_{l=1,l\neq k}^{K}|\boldsymbol{h}_k^{\mathrm{H}}\boldsymbol{F}_{\mathrm{R}}\boldsymbol{f}_{\mathrm{B},l}|^2+\boldsymbol{h}_k^{\mathrm{H}}\boldsymbol{F}_{\mathrm{R}}\boldsymbol{R}_{\mathrm{q}}\boldsymbol{F}_{\mathrm{R}}^{\mathrm{H}}\boldsymbol{h}_k+\sigma_k^2},k=1,2,\cdots,K. \tag{11}$$

but $\mathcal{H}_1$ holds. The detailed derivation of $\mathcal{P}_{\mathrm{e}}$ will be included in Section III.

C. Problem Formulation

With the derivation of (3) and (4), we can define SIQNR_k as the signal to interference, quantization distortion and noise ratio (SIQNR) for the kth user, which can be expressed as (11) at the top of this page. Then the SCR can be given by

$$R_{\mathrm{sum}}=\sum_{k=1}^{K}\log(1+\mathrm{SIQNR}_k). \tag{12}$$

To proceed, the optimization problem can be expressed as

$$\max_{\boldsymbol{F}_{\mathrm{R}},\boldsymbol{F}_{\mathrm{B}}}\ R_{\mathrm{sum}} \tag{13a}$$
$$\text{s.t.}\quad \big|[\boldsymbol{F}_{\mathrm{R}}]_{n,m}\big|=1,n=1,\cdots,N,m=1,\cdots,K, \tag{13b}$$
$$\mathbb{E}_{\boldsymbol{s}}\left(\Big\|\boldsymbol{F}_{\mathrm{R}}\big((1-\beta)\boldsymbol{F}_{\mathrm{B}}\boldsymbol{s}+\boldsymbol{\eta}_{\mathrm{q}}\big)\Big\|_{\mathrm{F}}^2\right)\leq P_{\max}, \tag{13c}$$
$$\mathbb{E}_{\boldsymbol{h}_{\mathrm{w}}}(\mathcal{P}_{\mathrm{e}})\geq 1-\epsilon, \tag{13d}$$

where ϵ is the predetermined level of covertness. (13b), (13c) and (13d) denote the constant modulus constraints on the elements of analog beamformer, the power constraint under the AQN model and the covertness constraint, respectively. Note that (13) is a non-convex problem and difficult to handle owing to the coupling of $\boldsymbol{F}_{\mathrm{R}}$ and $\boldsymbol{F}_{\mathrm{B}}$. To efficiently solve the problem, we will propose the AO scheme to design the hybrid beamformers in Section III.

III. AO SCHEME FOR HYBRID BEAMFORMER DESIGN

In this section, we will propose an AO scheme to solve (13). Specifically, the problem transformation is presented in Section III-A and the AO scheme for hybrid beamformer design is proposed in Section III-B.

A. Problem Transformation

We first derive the expression of the power constraint (13c). By substituting (3) into (13c) and using the fact that $\|\boldsymbol{A}\|_{\mathrm{F}}^2=\mathrm{Tr}(\boldsymbol{A}\boldsymbol{A}^{\mathrm{H}})$, (13c) can be transformed as

$$\mathrm{Tr}\Big(\boldsymbol{F}_{\mathrm{R}}\big((1-\beta)^2\sum_{l=1}^{K}\boldsymbol{f}_{\mathrm{B},l}\boldsymbol{f}_{\mathrm{B},l}^{\mathrm{H}}+\boldsymbol{R}_{\mathrm{q}}\big)\boldsymbol{F}_{\mathrm{R}}^{\mathrm{H}}\Big)\leq P_{\max}. \tag{14}$$

Then, we derive the expression of $\mathcal{P}_{\mathrm{e}}$ in (13d). Similar to [11], we assume that the blocklength is T, $T\gg 1$ and Willie can use T consecutive time slots to enhance its detection. Then we define

$$\mathbb{P}_1^T\triangleq\prod_{t=1}^{T}f(\boldsymbol{y}_{\mathrm{w}}[t]|\mathcal{H}_1), \tag{15}$$

$$\mathbb{P}_0^T\triangleq\prod_{t=1}^{T}f(\boldsymbol{y}_{\mathrm{w}}[t]|\mathcal{H}_0), \tag{16}$$

where $f(\boldsymbol{y}_{\mathrm{w}}[t]|\mathcal{H}_0)=\mathcal{CN}(\boldsymbol{0},\sigma_{\mathrm{w}}^2)$ and $f(\boldsymbol{y}_{\mathrm{w}}[t]|\mathcal{H}_1)=\mathcal{CN}\Big(\boldsymbol{0},\boldsymbol{h}_{\mathrm{w}}^{\mathrm{H}}\boldsymbol{F}_{\mathrm{R}}\big((1-\beta)^2\sum_{l=1}^{K}\boldsymbol{f}_{\mathrm{B},l}\boldsymbol{f}_{\mathrm{B},l}^{\mathrm{H}}+\boldsymbol{R}_{\mathrm{q}}\big)\boldsymbol{F}_{\mathrm{R}}^{\mathrm{H}}\boldsymbol{h}_{\mathrm{w}}+\sigma_{\mathrm{w}}^2\Big)$ denote the likelihood functions of $\boldsymbol{y}_{\mathrm{w}}$ under $\mathcal{H}_0$ and $\mathcal{H}_1$, respectively. To minimize the detection error probability $\widehat{\mathcal{P}}_{\mathrm{e}}$, Willie performs the optimal test [1] and $\widehat{\mathcal{P}}_{\mathrm{e}}$ can be derived as

$$\widehat{\mathcal{P}}_{\mathrm{e}}=1-\mathcal{V}(\mathbb{P}_1^T,\mathbb{P}_0^T), \tag{17}$$

where $\mathcal{V}(\mathbb{P}_1^T,\mathbb{P}_0^T)$ denotes the total variation distance between $\mathbb{P}_1^T$ and $\mathbb{P}_0^T$. Since it is difficult to further analyze the expressions of $\mathcal{V}(\mathbb{P}_1^T,\mathbb{P}_0^T)$, we can use the Pinsker's inequality [1] to obtain a tractable upper bound as

$$\mathcal{V}(\mathbb{P}_1^T,\mathbb{P}_0^T)\leq\sqrt{\frac{1}{2}\mathcal{D}(\mathbb{P}_1^T,\mathbb{P}_0^T)}, \tag{18}$$

where $\mathcal{D}(\mathbb{P}_1^T,\mathbb{P}_0^T)$ denotes the Kullback-Leibler (KL) divergence from $\mathbb{P}_1^T$ to $\mathbb{P}_0^T$. We first denote $\tau_0^2\triangleq\sigma_{\mathrm{w}}^2$ and $\tau_1^2\triangleq\boldsymbol{h}_{\mathrm{w}}^{\mathrm{H}}\boldsymbol{F}_{\mathrm{R}}\big((1-\beta)^2\sum_{l=1}^{K}\boldsymbol{f}_{\mathrm{B},l}\boldsymbol{f}_{\mathrm{B},l}^{\mathrm{H}}+\boldsymbol{R}_{\mathrm{q}}\big)\boldsymbol{F}_{\mathrm{R}}^{\mathrm{H}}\boldsymbol{h}_{\mathrm{w}}+\sigma_{\mathrm{w}}^2$. Then we can obtain

$$\begin{aligned}\mathcal{D}(\mathbb{P}_1^T,\mathbb{P}_0^T)&=\mathbb{E}_{\mathbb{P}_1}(T\ln\mathbb{P}_1-T\ln\mathbb{P}_0)\\&=T\Big(\ln\frac{\tau_0^2}{\tau_1^2}+\frac{\tau_1^2}{\tau_0^2}-1\Big).\end{aligned} \tag{19}$$

From Alice's perspective, considering (13d), (17) and (18), the covertness constraint can be replaced by

$$\mathbb{E}_{\boldsymbol{h}_{\mathrm{w}}}\Big(\sqrt{\frac{1}{2}\mathcal{D}(\mathbb{P}_1^T,\mathbb{P}_0^T)}\Big)\leq\epsilon. \tag{20}$$

By using the inequality $\xi-\ln(1+\xi)\leq\frac{\xi^2}{2},\forall\xi>0$ and letting $\xi=\frac{\tau_1^2}{\tau_0^2}-1$, we can derive an upper bound for the left hand of (20) to provide a safer scenario for covertness, which can be expressed as

$$\mathbb{E}_{\boldsymbol{h}_{\mathrm{w}}}\Big(\sqrt{\frac{1}{2}\mathcal{D}(\mathbb{P}_1^T,\mathbb{P}_0^T)}\Big)\leq\mathbb{E}_{\boldsymbol{h}_{\mathrm{w}}}\big(\frac{\sqrt{T}}{2}\xi\big)\leq\epsilon. \tag{21}$$

Subsequently, the covertness constraint can be transformed as

$$\mathrm{Tr}\bigg(\Big(\boldsymbol{F}_{\mathrm{R}}\big((1-\beta)^2\sum_{l=1}^{K}\boldsymbol{f}_{\mathrm{B},l}\boldsymbol{f}_{\mathrm{B},l}^{\mathrm{H}}+\boldsymbol{R}_{\mathrm{q}}\big)\boldsymbol{F}_{\mathrm{R}}^{\mathrm{H}}\Big)\boldsymbol{\Omega}_{\mathrm{w}}\bigg)\leq\frac{2\epsilon\sigma_{\mathrm{w}}^2}{\sqrt{T}}. \tag{22}$$

Therefore, the optimization problem can be expressed as

$$\max_{\boldsymbol{F}_{\mathrm{R}},\boldsymbol{F}_{\mathrm{B}}}\ R_{\mathrm{sum}} \tag{23a}$$
$$\text{s.t.}\quad (13\text{b}),(14),(22). \tag{23b}$$

As we can see, the objective is expressed as a sum of logarithmic functions of fractional items. Based on the quadratic and Lagrangian dual transform [12], we introduce auxiliary variables $\boldsymbol{r}\triangleq[r_1,r_2,\cdots,r_K]^{\mathrm{T}}$ and $\boldsymbol{z}\triangleq[z_1,z_2,\cdots,z_K]^{\mathrm{T}}$, then the equivalent form of the optimization problem (23) is given by (24) at the top of this page.

B. AO-based Hybrid Beamformer Design

Since it is difficult to optimize $\boldsymbol{F}_{\mathrm{R}},\boldsymbol{F}_{\mathrm{B}},\boldsymbol{r},\boldsymbol{z}$ simultaneously, we resort to the AO scheme [13] to solve (24). The detailed procedures are presented as follows.

$$\max_{\boldsymbol{F}_\mathrm{R},\boldsymbol{F}_\mathrm{B},\boldsymbol{r},\boldsymbol{z}} f_\mathrm{r}(\boldsymbol{F}_\mathrm{R},\boldsymbol{F}_\mathrm{B},\boldsymbol{r},\boldsymbol{z}) \triangleq \sum_{k=1}^{K}\Big(\log(1+r_k)-r_k+2(1-\beta)\sqrt{1+r_k}\mathrm{Re}(z_k^*\boldsymbol{h}_k^\mathrm{H}\boldsymbol{F}_\mathrm{R}\boldsymbol{f}_{\mathrm{B},k}) - |z_k|^2\big((1-\beta)^2\sum_{l=1}^{K}|\boldsymbol{h}_k^\mathrm{H}\boldsymbol{F}_\mathrm{R}\boldsymbol{f}_{\mathrm{B},l}|^2+\boldsymbol{h}_k^\mathrm{H}\boldsymbol{F}_\mathrm{R}\boldsymbol{R}_\mathrm{q}\boldsymbol{F}_\mathrm{R}^\mathrm{H}\boldsymbol{h}_k+\sigma_k^2\big)\Big) \tag{24a}$$

$$\text{s.t.}\quad (13\text{b}),(14),(22). \tag{24b}$$

$$\widehat{z}_k=\frac{(1-\beta)\sqrt{1+r_k}\boldsymbol{h}_k^\mathrm{H}\boldsymbol{F}_\mathrm{R}\boldsymbol{f}_{\mathrm{B},k}}{(1-\beta)^2\sum_{l=1}^{K}|\boldsymbol{h}_k^\mathrm{H}\boldsymbol{F}_\mathrm{R}\boldsymbol{f}_{\mathrm{B},l}|^2+\boldsymbol{h}_k^\mathrm{H}\boldsymbol{F}_\mathrm{R}\boldsymbol{R}_\mathrm{q}\boldsymbol{F}_\mathrm{R}^\mathrm{H}\boldsymbol{h}_k+\sigma_k^2}, k=1,2,\cdots,K. \tag{26}$$

1) Optimization for $\boldsymbol{r}$: When fixing $\boldsymbol{F}_\mathrm{R},\boldsymbol{F}_\mathrm{B},\boldsymbol{z}$, it can be seen f_r is a concave function of $\boldsymbol{r}$, thus the optimal $\widehat{r}_k$ can be obtained by letting $\partial f_\mathrm{r}/\partial r_k=0$ for $k=1,2,\cdots,K$ and can be expressed just like the form of SIQNR_k in (11), i.e.,

$$\widehat{r}_k=\mathrm{SIQNR}_k, k=1,2,\cdots,K. \tag{25}$$

2) Optimization for $\boldsymbol{z}$: When $\boldsymbol{F}_\mathrm{R},\boldsymbol{F}_\mathrm{B},\boldsymbol{r}$ are fixed, f_r is also a concave function of $\boldsymbol{z}$. Similarly, we let $\partial f_\mathrm{r}/\partial z_k=0$ for $k=1,2,\cdots,K$ and the optimal $\widehat{z}_k$ can be obtained as (26) at the top of this page.

3) Optimization for $\boldsymbol{F}_\mathrm{R}$: Given $\boldsymbol{F}_\mathrm{B},\boldsymbol{r},\boldsymbol{z}$, the optimization problem for $\boldsymbol{F}_\mathrm{R}$ can be expressed as

$$\max_{\boldsymbol{F}_\mathrm{R}} \sum_{k=1}^{K}\Big(2(1-\beta)\sqrt{1+r_k}\mathrm{Re}(z_k^*\boldsymbol{h}_k^\mathrm{H}\boldsymbol{F}_\mathrm{R}\boldsymbol{f}_{\mathrm{B},k}) - |z_k|^2\big((1-\beta)^2\sum_{l=1}^{K}|\boldsymbol{h}_k^\mathrm{H}\boldsymbol{F}_\mathrm{R}\boldsymbol{f}_{\mathrm{B},l}|^2+\boldsymbol{h}_k^\mathrm{H}\boldsymbol{F}_\mathrm{R}\boldsymbol{R}_\mathrm{q}\boldsymbol{F}_\mathrm{R}^\mathrm{H}\boldsymbol{h}_k\big)\Big) \tag{27a}$$

$$\text{s.t.}\quad (13\text{b}),(14),(22). \tag{27b}$$

The objective function in (27) related to $\boldsymbol{F}_\mathrm{R}$ can be transformed as

$$\begin{aligned}&\sum_{k=1}^{K}\Big(2(1-\beta)\sqrt{1+r_k}\mathrm{Re}(z_k^*\boldsymbol{h}_k^\mathrm{H}\boldsymbol{F}_\mathrm{R}\boldsymbol{f}_{\mathrm{B},k}) - |z_k|^2\big((1-\beta)^2\sum_{l=1}^{K}|\boldsymbol{h}_k^\mathrm{H}\boldsymbol{F}_\mathrm{R}\boldsymbol{f}_{\mathrm{B},l}|^2+\boldsymbol{h}_k^\mathrm{H}\boldsymbol{F}_\mathrm{R}\boldsymbol{R}_\mathrm{q}\boldsymbol{F}_\mathrm{R}^\mathrm{H}\boldsymbol{h}_k\big)\Big)\\ &\overset{(a)}{=}\sum_{k=1}^{K}\Bigg(2(1-\beta)\sqrt{1+r_k}\mathrm{Re}\big(z_k^*\mathrm{Tr}(\boldsymbol{f}_{\mathrm{B},k}\boldsymbol{h}_k^\mathrm{H}\boldsymbol{F}_\mathrm{R})\big) - |z_k|^2\bigg(\mathrm{Tr}\Big(\boldsymbol{F}_\mathrm{R}\big((1-\beta)^2\boldsymbol{F}_\mathrm{B}\boldsymbol{F}_\mathrm{B}^\mathrm{H}+\boldsymbol{R}_\mathrm{q}\big)\boldsymbol{F}_\mathrm{R}^\mathrm{H}\boldsymbol{h}_k\boldsymbol{h}_k^\mathrm{H}\Big)\bigg)\Bigg)\\ &\overset{(b)}{=}-\boldsymbol{f}_\mathrm{R}^\mathrm{H}\boldsymbol{Q}_0\boldsymbol{f}_\mathrm{R}-2\mathrm{Re}(\boldsymbol{p}_0^\mathrm{H}\boldsymbol{f}_\mathrm{R}),\end{aligned} \tag{28}$$

where

$$\boldsymbol{f}_\mathrm{R}\triangleq\mathrm{vec}(\boldsymbol{F}_\mathrm{R}), \tag{29}$$

$$\boldsymbol{Q}_0\triangleq\sum_{k=1}^{K}|z_k|^2\Big(\big((1-\beta)^2(\boldsymbol{F}_\mathrm{B}\boldsymbol{F}_\mathrm{B}^\mathrm{H})^\mathrm{T}+\boldsymbol{R}_\mathrm{q}^\mathrm{T}\big)\otimes(\boldsymbol{h}_k\boldsymbol{h}_k^\mathrm{H})\Big), \tag{30}$$

$$\boldsymbol{p}_0\triangleq-\sum_{k=1}^{K}(1-\beta)z_k\sqrt{1+r_k}(\boldsymbol{I}_K\otimes\boldsymbol{h}_k)\boldsymbol{f}_{\mathrm{B},k}^*. \tag{31}$$

Note that the equality (a) in (28) holds because $\mathrm{Tr}(\boldsymbol{AB})=\mathrm{Tr}(\boldsymbol{BA})$. The equality (b) holds due to the fact that $\mathrm{Tr}(\boldsymbol{A}^\mathrm{H}\boldsymbol{BC})=\big(\mathrm{vec}(\boldsymbol{A})\big)^\mathrm{H}(\boldsymbol{I}\otimes\boldsymbol{B})\mathrm{vec}(\boldsymbol{C})$ and $\mathrm{Tr}(\boldsymbol{ABA}^\mathrm{H}\boldsymbol{C})=\mathrm{vec}(\boldsymbol{A})^\mathrm{H}(\boldsymbol{B}^\mathrm{T}\otimes\boldsymbol{C})\mathrm{vec}(\boldsymbol{A})$.

Similarly, we can rewrite the constraints (14) and (22). Then, (27) can be equivalently transformed as

$$\min_{\boldsymbol{f}_\mathrm{R}} \boldsymbol{f}_\mathrm{R}^\mathrm{H}\boldsymbol{Q}_0\boldsymbol{f}_\mathrm{R}+2\mathrm{Re}(\boldsymbol{p}_0^\mathrm{H}\boldsymbol{f}_\mathrm{R}) \tag{32a}$$

$$\text{s.t.}\quad \boldsymbol{f}_\mathrm{R}^\mathrm{H}\boldsymbol{Q}_1\boldsymbol{f}_\mathrm{R}\le P_{\max}, \tag{32b}$$

$$\boldsymbol{f}_\mathrm{R}^\mathrm{H}\boldsymbol{Q}_2\boldsymbol{f}_\mathrm{R}\le\frac{2\epsilon\sigma_\mathrm{w}^2}{\sqrt{T}}, \tag{32c}$$

$$\big|[\boldsymbol{f}_\mathrm{R}]_u\big|=1, u=1,2,\cdots,KN, \tag{32d}$$

where

$$\boldsymbol{Q}_1\triangleq\big((1-\beta)^2(\boldsymbol{F}_\mathrm{B}\boldsymbol{F}_\mathrm{B}^\mathrm{H})^\mathrm{T}\big)\otimes\boldsymbol{I}_N, \tag{33}$$

$$\boldsymbol{Q}_2\triangleq\big((1-\beta)^2(\boldsymbol{F}_\mathrm{B}\boldsymbol{F}_\mathrm{B}^\mathrm{H})^\mathrm{T}\big)\otimes\boldsymbol{\Omega}_\mathrm{w}. \tag{34}$$

The newly obtained constraints (32b), (32c) and (32d) correspond to the original (14), (22) and (13b), respectively. Therefore, the problem in (32) is transformed into a standard QCQP problem with additional constant-modulus constraints, enabling us to solve it efficiently with the iMM method [14]. Once we obtain a feasible solution $\overline{\boldsymbol{f}}_\mathrm{R}$, the quadratic terms $\boldsymbol{f}_\mathrm{R}^\mathrm{H}\boldsymbol{Q}_v\boldsymbol{f}_\mathrm{R}$ for $v=1,2,3$ can be upper-bounded by

$$\boldsymbol{f}_\mathrm{R}^\mathrm{H}\boldsymbol{Q}_v\boldsymbol{f}_\mathrm{R}\le2\lambda_vKN+2\mathrm{Re}\big(\boldsymbol{f}_\mathrm{R}^\mathrm{H}(\boldsymbol{Q}_v-\lambda_v\boldsymbol{I}_N)\overline{\boldsymbol{f}}_\mathrm{R}\big)-\overline{\boldsymbol{f}}_\mathrm{R}^\mathrm{H}\boldsymbol{Q}\overline{\boldsymbol{f}}_\mathrm{R}, \tag{35}$$

where λ_v is usually selected as the maximum eigenvalue or the trace of $\boldsymbol{Q}_v$ to satisfy $\lambda_v\boldsymbol{I}_{KN}-\boldsymbol{Q}_v\succeq\boldsymbol{0}$. Therefore, we can derive a surrogate problem for (32) as

$$\min_{\boldsymbol{f}_\mathrm{R}} g_0(\boldsymbol{f}_\mathrm{R}) \tag{36a}$$

$$\text{s.t.}\quad g_v(\boldsymbol{f}_\mathrm{R})\le0, v=1,2, \tag{36b}$$

$$\big|[\boldsymbol{f}_\mathrm{R}]_u\big|=1, u=1,2,\cdots,KN, \tag{36c}$$

where we define

$$g_0(\boldsymbol{f}_\mathrm{R})\triangleq2\mathrm{Re}\Big(\boldsymbol{f}_\mathrm{R}^\mathrm{H}\big((\boldsymbol{Q}_0-\lambda_0\boldsymbol{I}_{KN})\overline{\boldsymbol{f}}_\mathrm{R}+\boldsymbol{p}_0\big)\Big) \tag{37}$$

$$g_1(\boldsymbol{f}_\mathrm{R})\triangleq2\mathrm{Re}\Big(\boldsymbol{f}_\mathrm{R}^\mathrm{H}\big((\boldsymbol{Q}_1-\lambda_1\boldsymbol{I}_{KN})\overline{\boldsymbol{f}}_\mathrm{R}\big)\Big)+2\lambda_1KN-\overline{\boldsymbol{f}}_\mathrm{R}^\mathrm{H}\boldsymbol{Q}_1\overline{\boldsymbol{f}}_\mathrm{R}-P_{\max}, \tag{38}$$

$$g_2(\boldsymbol{f}_{\rm R}) \triangleq 2{\rm Re}\Big(\boldsymbol{f}_{\rm R}^{\rm H}\big((\boldsymbol{Q}_2-\lambda_2\boldsymbol{I}_{KN})\overline{\boldsymbol{f}}_{\rm R}\big)\Big)+2\lambda_2 KN - \overline{\boldsymbol{f}}_{\rm R}^{\rm H}\boldsymbol{Q}_2\overline{\boldsymbol{f}}_{\rm R} - \frac{2\epsilon\sigma_{\rm w}^2}{\sqrt{T}}. \quad (39)$$

Since (36) is still non-convex due to (36c), we can solve its Lagrange dual problem which is expressed as

$$\sup_{\{\omega_1,\omega_2\geq 0\}} \min_{\{|[\boldsymbol{f}_{\rm R}]_u|=1\}_{u=1}^{KN}} g_0(\boldsymbol{f}_{\rm R}) + \sum_{v=1}^{2}\omega_v g_v(\boldsymbol{f}_{\rm R}). \quad (40)$$

Since the objective in (40) is a linear function of $\boldsymbol{f}_{\rm R}$, the optimal solution for $\boldsymbol{f}_{\rm R}$ can be given by

$$\widehat{\boldsymbol{f}}_{\rm R}(\omega_1,\omega_2) = \exp\bigg(j\angle\Big(\sum_{v=1}^{2}\big((\lambda_v\boldsymbol{I}_{KN}-\boldsymbol{Q}_v)\overline{\boldsymbol{f}}_{\rm R}\big)\omega_v + (\lambda_0\boldsymbol{I}_{KN}-\boldsymbol{Q}_0)\overline{\boldsymbol{f}}_{\rm R}\Big)\bigg). \quad (41)$$

Additionally, considering the remaining optimality conditions, i.e.,

$$g_v(\widehat{\boldsymbol{f}}_{\rm R}(\omega_1,\omega_2)) \leq 0, \omega_v \geq 0, v=1,2, \quad (42)$$

$$\omega_v g_v(\widehat{\boldsymbol{f}}_{\rm R}(\omega_1,\omega_2)) = 0, v=1,2, \quad (43)$$

we can alternately optimize the dual variables ω_1 and ω_2 until convergence. Based on [14, Lemma 3], the bisection method can be used to obtain the numerical results for ω_1 and ω_2. Using the converged dual variables, we can derive the optimal $\boldsymbol{f}_{\rm R}$ via (41).

4) Optimization for $\boldsymbol{F}_{\rm B}$: Given $\boldsymbol{F}_{\rm R}, \boldsymbol{r}, \boldsymbol{z}$, we now optimize $\boldsymbol{F}_{\rm B}$. We first define $\boldsymbol{f}_{\rm B} \triangleq {\rm vec}(\boldsymbol{F}_{\rm B})$ and introduce a series of auxiliary matrices shown as

$$\boldsymbol{S}_l \triangleq [\overbrace{\boldsymbol{0},\cdots,\boldsymbol{0}}^{l-1}, \boldsymbol{I}_K, \overbrace{\boldsymbol{0},\cdots,\boldsymbol{0}}^{K-l}], l=1,2,\cdots,K \quad (44)$$

to satisfy that $[\boldsymbol{F}_{\rm B}]_{:,k} = \boldsymbol{S}_k\boldsymbol{f}_{\rm B}$ for $k=1,2,\cdots,K$. Then we can transform the optimization problem for $\boldsymbol{f}_{\rm B}$ as

$$\min_{\boldsymbol{f}_{\rm B}} \ \boldsymbol{f}_{\rm B}^{\rm H}\boldsymbol{\Xi}_0\boldsymbol{f}_{\rm B} + 2{\rm Re}(\boldsymbol{\phi}_0^{\rm H}\boldsymbol{f}_{\rm B}) \quad (45a)$$

$$\text{s.t.} \ \ \boldsymbol{f}_{\rm R}^{\rm H}\boldsymbol{\Xi}_1\boldsymbol{f}_{\rm R} \leq P_{\max}, \quad (45b)$$

$$\boldsymbol{f}_{\rm R}^{\rm H}\boldsymbol{\Xi}_2\boldsymbol{f}_{\rm R} \leq \frac{2\epsilon\sigma_{\rm w}^2}{\sqrt{T}}, \quad (45c)$$

where

$$\boldsymbol{\phi}_0 \triangleq -\sum_{k=1}^{K}\big((1-\beta)z_k\sqrt{1+r_k}\boldsymbol{S}_k^{\rm H}\boldsymbol{F}_{\rm R}^{\rm H}\boldsymbol{h}_k\big), \quad (46)$$

$$\boldsymbol{\Xi}_0 \triangleq \sum_{k=1}^{K}|z_k|^2\Big(\sum_{l=1}^{K}\big((1-\beta)^2\boldsymbol{S}_l^{\rm H}\boldsymbol{F}_{\rm R}^{\rm H}\boldsymbol{h}_k\boldsymbol{h}_k^{\rm H}\boldsymbol{F}_{\rm R}\boldsymbol{S}_l + \beta(1-\beta)\boldsymbol{S}_l^{\rm H}{\rm diag}(\boldsymbol{F}_{\rm R}^{\rm H}\boldsymbol{h}_k\boldsymbol{h}_k^{\rm H}\boldsymbol{F}_{\rm R})\boldsymbol{S}_l\big)\Big), \quad (47)$$

$$\boldsymbol{\Xi}_1 \triangleq \sum_{k=1}^{K}\boldsymbol{S}_k^{\rm H}\big((1-\beta)^2\boldsymbol{F}_{\rm R}^{\rm H}\boldsymbol{F}_{\rm R} + \beta(1-\beta){\rm diag}(\boldsymbol{F}_{\rm R}^{\rm H}\boldsymbol{F}_{\rm R})\big)\boldsymbol{S}_k, \quad (48)$$

$$\boldsymbol{\Xi}_2 \triangleq \sum_{k=1}^{K}\boldsymbol{S}_k^{\rm H}\big((1-\beta)^2\boldsymbol{F}_{\rm R}^{\rm H}\boldsymbol{\Omega}_{\rm w}\boldsymbol{F}_{\rm R} + \beta(1-\beta){\rm diag}(\boldsymbol{F}_{\rm R}^{\rm H}\boldsymbol{\Omega}_{\rm w}\boldsymbol{F}_{\rm R})\big)\boldsymbol{S}_k\big). \quad (49)$$

Algorithm 1 AO-based Hybrid Beamformer Design.

1: **Input**: $\boldsymbol{h}_1,\cdots,\boldsymbol{h}_K$, $\boldsymbol{\Omega}_{\rm w}$, $P_{\max}$, ϵ.
2: Initialize $\boldsymbol{F}_{\rm R}$, $\boldsymbol{F}_{\rm B}$.
3: **repeat**
4: Update $r_k, k=1,2,\cdots,K$ via (25).
5: Update $z_k, k=1,2,\cdots,K$ via (26).
6: Update analog beamformer $\boldsymbol{f}_{\rm R}$ by solving (32).
7: Update digital beamformer $\boldsymbol{f}_{\rm B}$ by solving (45).
8: **until** $f_{\rm r}$ in (24) is converged.
9: **Output**: $\boldsymbol{F}_{\rm R} = {\rm vec}^{-1}(\boldsymbol{f}_{\rm R})$, $\boldsymbol{F}_{\rm B} = {\rm vec}^{-1}(\boldsymbol{f}_{\rm B})$.

Since $\boldsymbol{\Xi}_0, \boldsymbol{\Xi}_1$ and $\boldsymbol{\Xi}_2$ are all Hermitian semi-definite matrices, (45) is a standard QCQP convex problem, which can be solved by existing optimization toolbox.

Finally, We summarize the proposed AO scheme for hybrid beamformer design in **Algorithm** 1.

IV. Simulation Results

In this section, we evaluate the performance of the proposed AO scheme. We suppose that Alice is equipped with $N=64$ antennas and $N_{\rm RF}=4$ RF chains serving $K=4$ legitimate users. The channels between Alice and each legitimate user (or Willie) are all established with $D=3$ channel paths with a LOS path and two NLOS paths. Specifically, we assume that the channel gain of the LOS path obeys $\alpha^{(0)} \sim \mathcal{CN}(0,1)$, the other two channel gains of NLOS paths obey $\alpha^{(1)} \sim \mathcal{CN}(0,0.01)$ and $\alpha^{(2)} \sim \mathcal{CN}(0,0.001)$ [15]. The maximal transmission power is $P_{\max}=0$ dBw and the noise powers are $\sigma_1^2=\sigma_2^2=\cdots=\sigma_K^2=\sigma_{\rm w}^2=10$ dBm.

Fig. 1 illustrates the SCR versus different predetermined detection error probabilities, where we compare the performance of our proposed AO scheme for three cases including $b=1$, 4 and 7. For comparisons, we consider two baseline schemes: 1) Fully-digital beamformer optimization (FDBO) scheme that we design a fully-digital beamformer $\boldsymbol{F}\in\mathbb{C}^{N\times K}$ with a revised AO scheme in **Algorithm** 1 by removing the analog beamformer design and revising the dimension of the digital beamformer. 2) Maximum ratio transmitting (MRT) scheme that we design a fully-digital beamformer $\boldsymbol{F}\in\mathbb{C}^{N\times K}$ commonly used for covertness analysis, where $\boldsymbol{F}=\sqrt{p}\boldsymbol{H}^{\rm H}$ and p is normalized to satisfy both power and covertness constraints. It can be observed that our proposed AO scheme outperforms the MRT scheme. Additionally, when quantization noise is negligible at $b=7$, the AO scheme can achieve the performance comparable to that of the FDBO scheme. Moreover, the AO scheme demonstrates superior stability against variations in covertness constraints compared to the FDBO scheme at $b=1$. The reason is that the extra analog beamforming in the hybrid architecture reduces the leakage of quantization noise in the Alice-Willie link so that the transmit power can be utilized as fully as possible without exceeding $P_{\max}$ to achieve better SCR performance.

In Fig. 2, we evaluate the SCR performance as a function of b to illustrate the impact of the quantized bits of DACs. It

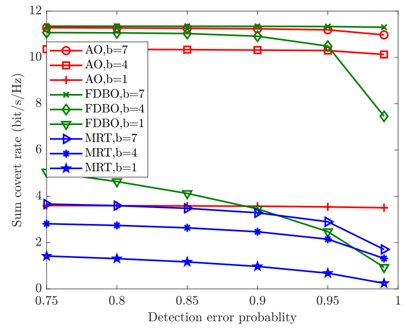

Fig. 1. Comparisons of the SCR for different schemes with varying detection error probabilities.

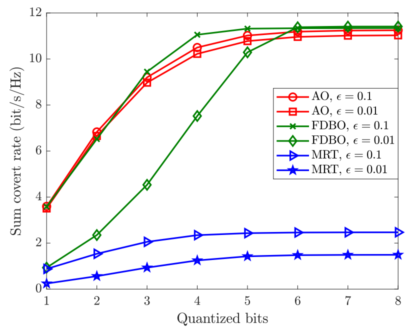

Fig. 2. Comparisons of the SCR for different schemes with varying quantized bits.

can be observed that as b increases, the SCR performance first improves when $b \leq 5$ and then tends to be flat when $b > 5$. This phenomenon occurs because that the quantization noise decreases rapidly with increasing b. Additionally, the result shows that our proposed AO scheme exhibits lower sensitivity to the covertness than the FDBO scheme.

Fig. 3 illustrates the SCR performance versus different numbers of the legitimate users. As K increases, both the FDBO and the AO schemes demonstrate an improvement in SCR performance, whereas the MRT scheme exhibits a decline. The reason is that the MRT scheme does not consider the covertness, multiuser interference, and quantization noise suppression, different from the other two schemes. Furthermore, the AO scheme can outperform the FDBO scheme when $K > 3$ in the case of low-resolution DACs, e.g., $b = 1$, due to smaller quantization noise in the hybrid beamforming architecture.

V. Conclusion

In this paper, we have investigated the hybrid beamformer design for covert mmWave MIMO communications with finite-resolution DACs. For future research, we will extend our work to the wideband mmWave MIMO communications.

VI. Acknowledgment

This work is supported in part by National Natural Science Foundation of China (NSFC) under Grants U22B2007 and 62071116, and by National Key Research and Development Program of China under Grant 2021YFB2900404.

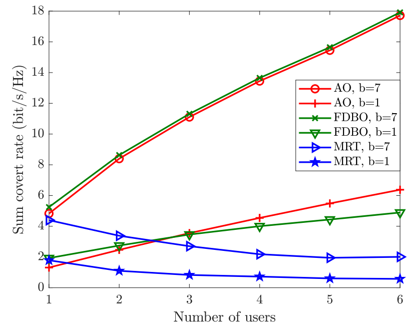

Fig. 3. Comparisons of the SCR for different schemes with varying numbers of users.

References

[1] B. A. Bash, D. Goeckel, and D. Towsley, "Limits of reliable communication with low probability of detection on AWGN channels," *IEEE J. Sel. Areas Commun.*, vol. 31, no. 9, pp. 1921–1930, Sep. 2013.

[2] D. Goeckel, B. Bash, S. Guha, and D. Towsley, "Covert communications when the warden does not know the background noise power," *IEEE Commun. Lett.*, vol. 20, no. 2, pp. 236–239, Feb. 2016.

[3] K. Shahzad, X. Zhou, and S. Yan, "Covert communication in fading channels under channel uncertainty," in *Proc. IEEE 85th Veh. Technol. Conf. (VTC Spring)*, Sydney, NSW, Australia, June 2017, pp. 1–5.

[4] Z. Xing, C. Qi, Y. Cheng, Y. Wu, D. Lv, and P. Li, "Covert millimeter wave communications based on beam sweeping," *IEEE Commun. Lett.*, vol. 27, no. 5, pp. 1287–1291, May 2023.

[5] S. Ma *et al.*, "Robust beamforming design for covert communications," *IEEE Trans. Inf. Forensics Security*, vol. 16, pp. 3026–3038, 2021.

[6] K. Chen, C. Qi, and G. Y. Li, "Two-step codeword design for millimeter wave massive MIMO systems with quantized phase shifters," *IEEE Trans. Signal Process.*, vol. 68, pp. 170–180, Dec. 2020.

[7] C. Qi, J. Hu, Y. Du, and A. Nallanathan, "Multiuser beamforming for partially-connected millimeter wave massive MIMO," *IEEE Trans. Veh. Technol.*, vol. 73, no. 4, pp. 5977–5981, Apr. 2024.

[8] C. Wang, Z. Li, and D. W. K. Ng, "Covert rate optimization of millimeter wave full-duplex communications," *IEEE Trans. Wireless Commun.*, vol. 21, no. 5, pp. 2844–2861, May 2022.

[9] W. B. Abbas, F. Gomez-Cuba, and M. Zorzi, "Millimeter wave receiver efficiency: A comprehensive comparison of beamforming schemes with low resolution ADCs," *IEEE Trans. Wireless Commun.*, vol. 16, no. 12, pp. 8131–8146, Dec. 2017.

[10] K. Roth and J. A. Nossek, "Achievable rate and energy efficiency of hybrid and digital beamforming receivers with low resolution ADC," *IEEE J. Sel. Areas Commun.*, vol. 35, no. 9, pp. 2056–2068, Sep. 2017.

[11] Y. Zhang, W. Ni, Y. Mao, B. Ning, S. Xiao, W. Tang, and D. Niyato, "Rate-splitting multiple access for covert communications," *IEEE Wireless Commun. Lett.*, vol. 13, no. 6, pp. 1685–1689, June 2024.

[12] K. Shen and W. Yu, "Fractional programming for communication systems—Part II: Uplink scheduling via matching," *IEEE Trans. Signal Process.*, vol. 66, no. 10, pp. 2631–2644, May 2018.

[13] C. Qi, Q. Liu, X. Yu, and G. Y. Li, "Hybrid precoding for mixture use of phase shifters and switches in mmWave massive MIMO," *IEEE Trans. Commun.*, vol. 70, no. 6, pp. 4121–4133, June 2022.

[14] X. He and J. Wang, "QCQP with extra constant modulus constraints: Theory and application to SINR constrained mmWave hybrid beamforming," *IEEE Trans. Signal Process.*, vol. 70, pp. 5237–5250, 2022.

[15] K. Chen, C. Qi, C.-X. Wang, and G. Y. Li, "Beam training and tracking for extremely large-scale MIMO communications," *IEEE Trans. Wireless Commun.*, vol. 23, no. 5, pp. 5048–5062, May 2024.